Am J Physiol Gastrointest Liver Physiol 293: G1300–G1307, 2007.
First published October 11, 2007; doi:10.1152/ajpgi.00422.2007.

SMIT2 mediates all myo-inositol uptake in apical membranes of rat small intestine

Rym Aouameur,[1] Sandra Da Cal,[1] Pierre Bissonnette,[1] Michael J. Coady,[1] and Jean-Yves Lapointe[1,2]

[1]*Groupe d'étude des protéines membranaires (GÉPROM), Département de Physiologie and* [2]*Département de Physique, Université de Montréal, Montréal, Québec, Canada*

Submitted 18 September 2007; accepted in final form 11 October 2007

Aouameur R, Da Cal S, Bissonnette P, Coady MJ, Lapointe J-Y. SMIT2 mediates all myo-inositol uptake in apical membranes of rat small intestine. *Am J Physiol Gastrointest Liver Physiol* 293: G1300–G1307, 2007. First published October 11, 2007; doi:10.1152/ajpgi.00422.2007.—This study presents the characterization of myo-inositol (MI) uptake in rat intestine as evaluated by use of purified membrane preparations. Three secondary active MI cotransporters have been identified; two are Na^+ coupled (SMIT1 and SMIT2) and one is H^+ coupled (HMIT). Through inhibition studies using selective substrates such as D-chiro-inositol (DCI, specific for SMIT2) and L-fucose (specific for SMIT1), we show that SMIT2 is exclusively responsible for apical MI transport in rat intestine; rabbit intestine appears to lack apical transport of MI. Other sugar transport systems known to be present in apical membranes, such as SGLT1 or GLUT5, lacked any significant contribution to MI uptake. Functional analysis of rat SMIT2 activity, via electrophysiological studies in *Xenopus* oocytes, demonstrated similarities to the activities of SMIT2 from other species (rabbit and human) displaying high affinities for MI (0.150 ± 0.040 mM), DCI (0.31 ± 0.06 mM), and phlorizin (Pz; 0.016 ± 0.007 mM); low affinity for glucose (36 ± 7 mM); and no affinity for L-fucose. Although these functional characteristics essentially confirmed those found in rat intestinal apical membranes, a unique discrepancy was seen between the two systems studied in that the affinity constant for glucose was ~40-fold lower in vesicles (K_i = 0.94 ± 0.35 mM) than in oocytes. Finally, the transport system responsible for the basolateral efflux transporter of glucose in intestine, GLUT2, did not mediate any significant radiolabeled MI uptake in oocytes, indicating that this transport system does not participate in the basolateral exit of MI from small intestine.

brush border; glucose; transport; oocytes; phlorizin

THE PHYSIOLOGICAL IMPORTANCE of myo-inositol (MI) is generally considered to reflect its role in signal transduction as a precursor to phosphoinositides and inositol phosphates. In addition, MI acts as a "compatible osmolyte" in specific tissues, such as brain and kidney medulla, where variations in milieu osmolarity may threaten normal cell function. In response to an increase in osmolarity, intracellular MI concentration may rise up to 500-fold above its plasma concentration of ~30 μM (9, 11, 12), where it prevents the accumulation effects of high ionic concentrations, which leads to DNA degradation (11a). This has been well documented in brain where conditions such as trauma (30), edema and hypernatremia (26, 27, 38) have been shown to increase MI levels. To reach such high intracellular concentrations, secondary active transport systems are required for MI.

Three such MI cotransport systems have been identified, two of which are sodium dependent (SMIT1 and SMIT2) whereas the third is proton dependent (HMIT) (36). SMIT1, the first MI transport system identified, is primarily expressed in brain and renal medulla (22). In the kidney (where MI transport has been most extensively studied), the protein is located at the basolateral membranes of epithelial cells (2, 39) and its activity is tightly regulated by osmotic variations through a tonicity-responsive system (16, 20). This regulation is most important in renal medulla where the interstitial osmolarity fluctuates drastically according to hydration status.

More recently, our laboratory has identified a second sodium-dependent transporter SMIT2 (10). Like SMIT1, SMIT2 is expressed in the brain, intestine, and kidney, and, although both systems share remarkable functional similarities (high affinities for MI, overall substrate and inhibitor specificities, and 2:1 Na^+-MI stoichiometry), some differences distinguish the two transport systems: unlike SMIT1, which is highly expressed in the kidney medulla, SMIT2 is predominantly found in kidney cortex where it is expressed at the apical domains of proximal tubule cells (2, 23). With this cellular location, SMIT2 is believed to be responsible for the reabsorption of MI from the glomerular filtrate, a conclusion that has been supported by MI uptake studies performed both on purified rabbit kidney brush border membrane vesicles (BBMv) (23) and on a stably SMIT2-transfected cell line (MDCK-SMIT2) (2). As well, there is no evidence that SMIT2 is regulated by osmolarity conditions, which is in accordance with its cortical location in kidney. A significant difference between the two SMIT transport systems concerns D-chiro-inositol (DCI), a MI epimer that is transported by SMIT2 with high affinity but is not transported by SMIT1 (10). In contrast, L-fucose is transported by SMIT1 but not by SMIT2. For these reasons, DCI and L-fucose can be used to functionally discriminate the two systems in tissues where they coexist (2).

A study performed on purified rat intestinal BBMv prior to the molecular identification of SMIT1 suggested the existence of a sodium-dependent MI transport system (34). In agreement with this conclusion, the dietary requirement for MI was first established by using gerbils, linking an MI-free diet to pathological conditions such as lipodystrophy of the small intestine, presumably because of failure in lipid absorption through chylomicrons (7, 18), and dysregulation of triglyceride metabolism in the liver (19). Using purified BBMv, we now demonstrate through extensive characterization that, in the rat, SMIT2 is present in the apical membranes of enterocytes and

Address for reprint requests and other correspondence: J.-Y. Lapointe, Groupe d'étude des protéines membranaires (GÉPROM), Université de Montréal, C.P. 6128, Succ. Centre-Ville, Montréal, Québec, Canada, H3C 3J7 (e-mail: jean-yves.lapointe@umontreal.ca).

The costs of publication of this article were defrayed in part by the payment of page charges. The article must therefore be hereby marked "*advertisement*" in accordance with 18 U.S.C. Section 1734 solely to indicate this fact.

is responsible for all MI absorption. This is in contrast to a recently published hypothesis that SMIT2 may play a significant role in glucose uptake in intestine (37).

MATERIALS AND METHODS

Materials

Radiolabeled [^{3}H]2-MI and [^{3}H]6-glucose were purchased from Perkin-Elmer (Boston, MA) and nitrocellulose filters for uptake assays were from Millipore (Billerica, MA). Trizol reagent, DNA primers, and Superscript III Platinum One-Step kit for quantitative real-time PCR (qRT-PCR) were purchased from Invitrogen (Carlsbad, CA). Other biochemicals were purchased from either Fisher Scientific (Ottawa, ON, Canada) or Sigma (Oakville, ON, Canada). Rats (Sprague-Dawley, 150–200 g) and rabbits (New Zealand White male, 2 kg) were purchased from Charles River Laboratories (St-Constant, QC, Canada). All animal manipulations were performed in accordance with the Canadian guidelines and were approved by the ethics committee of the Université de Montréal.

Isolation of Purified Brush Border Membranes

Brush border membranes from rat and rabbit intestinal mucosal scrapings were purified as described earlier for rabbit kidney (2). The membranes were prepared in batches using 6–10 rats (or 2–3 rabbits) and used fresh or kept frozen in liquid nitrogen until use (stored <4 wk). The composition of the intravesicular medium consisted of (in mM) 200 KCl, 0.1 $MgSO_4$, 300 mannitol, and 50 HEPES-Tris pH 7.0.

Cloning of Rat SMIT2 Coding Sequence

Rat SMIT2 cDNA was obtained by performing reverse transcription of rat renal mRNA with Superscript II according to the manufacturer's instructions (Invitrogen, Burlington, ON, Canada) followed by PCR using Phusion Polymerase (Fermentas, Burlington, ON, Canada). The oligonucleotides used were GATCTGCAGACCGACTGAGAAGTCATTCAG for the 5′ primer and CTAGTAAACACACAGCTTTATTATCGTTTCCTGG for the 3′ primer. The PCR product was treated with Exonuclease III (21) and inserted into the vector pT7TS, which had previously been cleaved with *Bgl* II and *Spe* I. After cloning, the recombinant vector was purified and then cleaved with *Eco*R I; mRNA was transcribed by using the T7 mMessage mMachine kit from Ambion (Austin, TX).

Oocyte Preparation, Injection of cRNA, and Incubation

Procedures for oocytes isolated from *Xenopus laevis* were as previously described (2). On the day following isolation, oocytes were injected with either 46 ng human GLUT2 mRNA (46 nl at 1 μg/μl) (13) for 2-deoxyglucose (2DG) uptake assays or 4.6 ng rat SMIT2 mRNA (46 nl at 0.1 μg/μl) for electrophysiology studies and incubated in Barth's solution supplemented with 5% horse serum, 2.5 mM Na pyruvate, and antibiotics (penicillin, streptomycin, and kanamycin) for 5–7 days prior to assay.

Electrophysiology

Oocyte currents were measured with a two-microelectrode voltage-clamp technique as previously described (4). Current and voltage electrodes were filled with 1 M KCl, and resistances were between 4 and 14 MΩ. The bath reference and current electrodes were Ag/AgCl pellets. The oocyte bath was continuously perfused with a modified low-sodium Barth's solution (65 mM NaCl instead of 90 mM along with 50 mM mannitol to maintain osmolarity). Only oocytes with resting potentials more negative than −30 mV were employed. The pulse protocol consisted of eight successive pulses of 250 ms separated by 500-ms periods at the resting potential (−50 mV), covering a voltage range of +50 to −125 mV in 25-mV increments. Current and voltage data were analyzed by averaging values in a 25-ms window starting at 210 ms after initiation of the pulse. For determination of kinetic parameters, MI and DCI were added to low-sodium Barth's solution in varying concentrations (0.01, 0.03, 0.1, 0.3, and 1 mM). The media used for kinetic evaluation of glucose employed glucose concentrations up to 50 mM by performing equimolar replacement of mannitol. For determination of phlorizin (Pz) affinity, the inhibitor was present in concentrations up to 1 mM.

Transport Studies

On BBMv. Uptake of radiolabeled MI was performed as described elsewhere by a standard filtration technique (23). Transport was initiated by mixing freshly thawed BBMv with transport media in a 1:10 ratio (in mM: 200 NaCl, 0.1 $MgSO_4$, 300 mannitol, 50 HEPES-Tris pH 7, and 1 μCi/ml [^{3}H]MI) at room temperature. When required for osmolarity balance (variations >5 mM), addition of substrates was compensated by removal of equivalent molar quantities of mannitol. After set intervals, 50-μl samples were rapidly filtered on 65-μm nitrocellulose filters and rinsed with 5 ml of ice-cold substrate-free transport media. Alternatively, a Fast Sampling, Rapid Filtration apparatus was used to perform very brief uptakes (1). Filters were then dissolved in 5 ml of scintillation cocktail (Betablend, ICN Biochemicals), and radioactivity was monitored with a Beckman LS6000 SC scintillation counter.

On oocytes. Uptakes were performed as already described (2). Control or GLUT2-injected oocytes were tested for both 2DG and MI uptake. Oocytes were incubated in Barth's solution containing tracer amount of substrate (1 μl/ml [^{3}H]MI or [^{3}H]2DG) with or without saturating cold substrate (10 mM MI or 2DG) to separate specific and nonspecific uptake.

qRT-PCR

Quantification of SMIT2 mRNA was performed by using LUX technology employing a SuperScript III Platinum one-step qRT-PCR system kit (Invitrogen). Total RNA was isolated from kidney cortices and intestinal mucosa from rats and rabbits by the Trizol extraction procedure. Both rabbit and rat SMIT2 mRNA were used as standards for quantification of specific mRNAs by procedures described elsewhere (23).

Data Analysis

Determination of kinetic parameters was performed by using Origin 6.1 software (OriginLab, Northampton, MA). For radiolabeled uptakes into BBMv, values are presented as pmol/mg protein for various time intervals. K_m values for MI were determined by use of a tracer inhibition equation described elsewhere (28) whereas K_i values for DCI and D-glucose were performed by using the classical competitive inhibition equation with predetermined K_m and V_{max} values for MI set as constant parameters. For electrophysiological studies, determination of kinetic parameters for MI, DCI, and glucose was performed by fitting data to the Michaelis-Menten equation without a nonspecific component. Evaluation of the K_i value for Pz was performed by fitting data to a competitive inhibition equation using K_m and I_{max} values for MI as constant parameters. The uncertainties described for the calculated parameters represent the accuracy of the fitting procedure as determined by the software. All experiments were performed at least three times using three different BBMv or oocyte preparations. Figures represent typical results.

RESULTS

MI Transport in Intestinal BBMv

Past studies of transporters using BBMv purified from both intestine and kidney were often performed using rabbits because they provide large quantities of material and a high

degree of purification. In a previous paper from our laboratory, BBMv purified from rabbit kidney were successfully used to characterize the luminal transport of MI (23). A similar set of experiments was thus performed to investigate MI uptake processes in the rabbit intestine. Figure 1*A* depicts uptake-time curves for MI in BBMv in either the presence (○) or absence (●) of saturating amounts of cold substrate (10 mM). To our surprise, all experiments using rabbit intestine (8 assays) failed to show typical uptake curves comprising overshoot and rapid settling back to equilibrium level, although two assays did present a twofold increase of tracer MI uptake over that seen under saturating conditions. On the other hand, BBMv purified from rat small intestine (Fig. 1*B*) showed high levels of specific MI uptake. As shown, a typical overshoot indicative of secondary active transport systems is found under tracer conditions whereas simple equilibration is achieved if 10 mM cold MI is present in the uptake media. The overshoot was observed for the first minute of uptake and the amount of intravesicular, radiolabeled MI attained over four times the equilibrium level, which was reached within 10 min. Such a clear distinction between the MI uptake seen with rabbit and rat led us to quantify the presence of SMIT2 transporters in kidney and intestine for both rat and rabbit. As shown in Fig. 2, quantification of SMIT2 mRNA through qRT-PCR shows equivalent expression levels in rat for both kidney and intestine whereas in rabbit only the kidney expresses SMIT2 mRNA with barely any SMIT2 detection in intestine.

Characterization of MI Transport in Purified Rat BBMv

Because rabbit intestine lacked any specific MI uptakes, we used rat BBMv to clearly identify the nature of the transporter(s) involved and to define the kinetics of MI transport activities. Descriptive characterization of MI transport was achieved by performing initial MI uptakes (15 s) in the presence of known substrates and/or inhibitors of the two SMIT subtypes. This complete characterization is presented in Fig. 3. Initial uptakes of radiolabeled MI (0.16 pmol/mg protein × 15 s) were challenged by different concentrations of the following agents: cold MI and glucose (up to 2 mM), DCI and Pz (up to 1 mM). The initial uptake (Ctrl) was also performed in the absence of sodium (K^+ replacement) to identify any possible Na^+-independent pathway for MI in BBMv. In addition, MI uptake was tested with the glucose facilitated transport inhibitor phloretin (Pt, 1 mM), L-fucose (100 mM), the GLUT-specific substrate 2DG (10 mM) and with the SGLT1-specific substrate α-methylglucose (AMG, 10 mM).

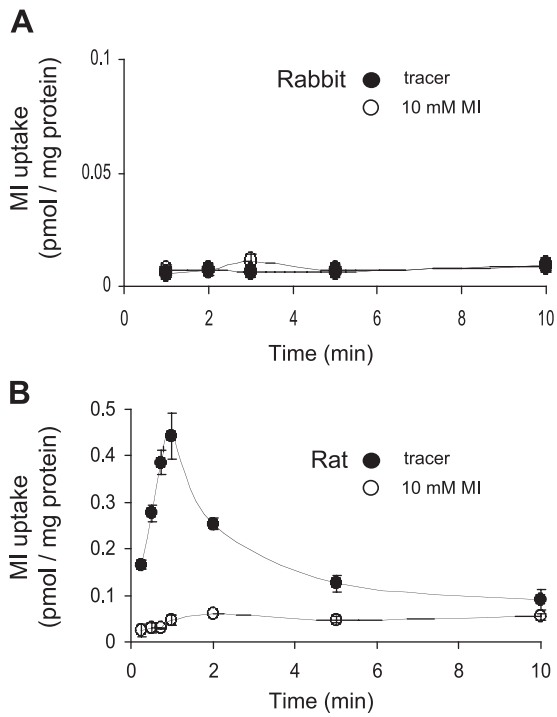

Fig. 1. Uptake of tracer myo-inositol (MI) into purified brush border membrane vesicles (BBMv). Tracer MI (0.36 nM) with (○) or without (●) saturating cold substrate (10 mM MI) was incubated with BBMv purified from rabbit (*A*) or rat (*B*) small intestine. Data represent means ± SE of triplicates.

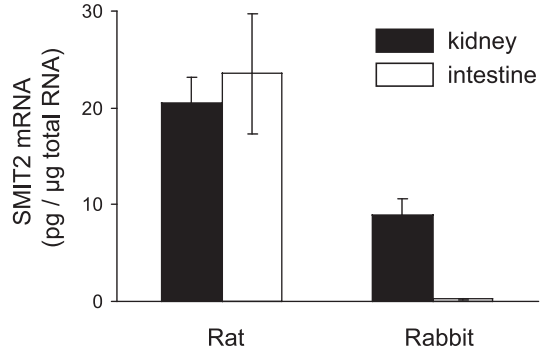

Fig. 2. Quantification of SMIT2 mRNA in kidney and intestine. mRNA purified from kidney (solid bar) and intestine (open bar) from both rat and rabbit were quantified for SMIT2 by quantitative real-time PCR (qRT-PCR; see MATERIALS AND METHODS). Data represent means ± SE of triplicates from 3 individuals.

As expected, all MI accumulation within the BBMv was completely Na^+ dependent given that uptake in the absence of sodium was similar to that found in the presence of excess cold MI. Furthermore, since increasing amounts of DCI completely inhibited specific MI uptake whereas 100 mM L-fucose failed to reduce uptake significantly, it can be concluded that there is no evidence for any SMIT1 activity in rat BBMv whereas SMIT2 (the DCI-sensitive transporter) appeared to be responsible for all MI transport observed. As expected from the properties of rabbit SMIT2 (28), 50 μM Pz was efficient in inhibiting MI uptake whereas Pt was without effect. Furthermore, the SGLT1 and GLUT transport systems showed no evidence of being involved in BBMv MI transport since high concentrations of their specific substrates (AMG and 2DG, respectively) failed to alter initial uptake of 0.36 nM MI. It is interesting that 1 mM D-glucose is effective in reducing the level of MI transport whereas 10 mM AMG fails to inhibit MI transport significantly. This is consistent with the reported properties of rabbit SMIT2 in which 50 mM AMG did not stimulate a cotransport current but 50 mM D-glucose did (10). We thus conclude that, in rat intestine, SMIT2 is the only transport system involved in the apical uptake of MI.

In the next set of experiments, inhibition curves were used to evaluate kinetic parameters using an analysis technique based on the competitive inhibition of tracer uptake either by its own substrate or by true competitive inhibitors (28). K_m and V_{max} values were thus first determined for MI and were then set as constant parameters for the evaluation of K_i values for all other

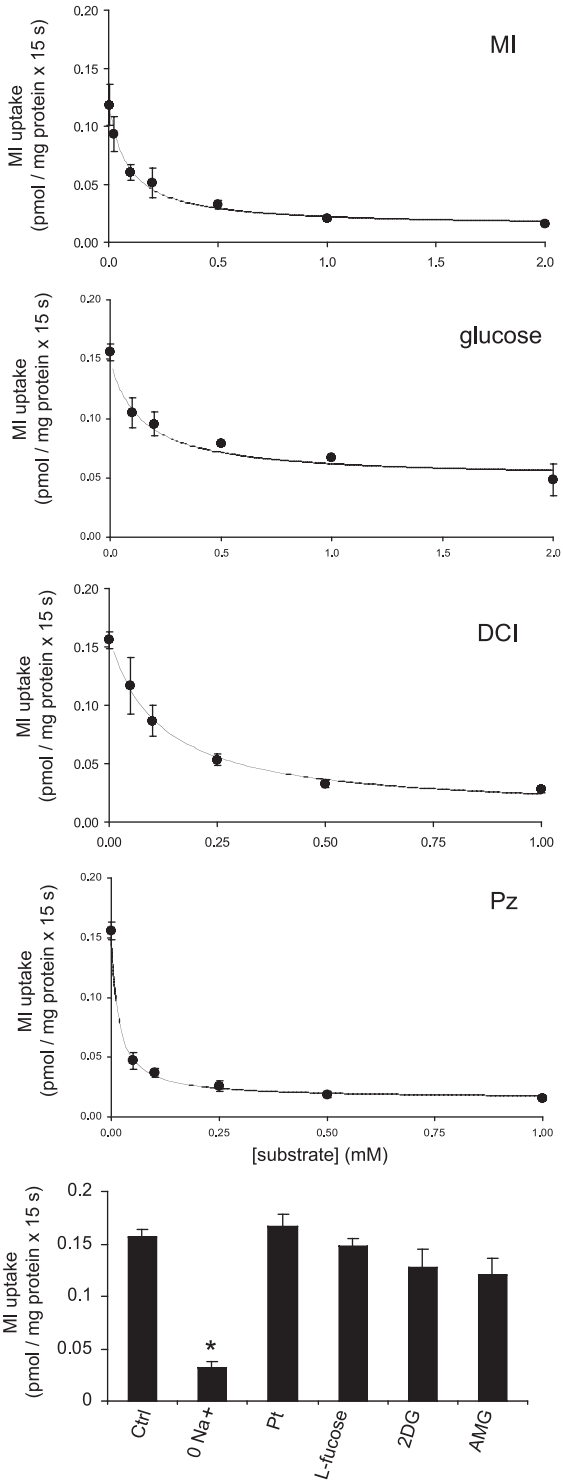

Fig. 3. Inhibition profile of tracer MI uptake on purified rat BBMv. Purified BBMv were incubated for 15 s with tracer MI (0.36 nM) in the presence of different concentrations of various agents [MI, glucose, D-chiro-inositol (DCI), and phlorizin (Pz)] and uptakes are shown as displacement curves. Also, similar inhibition assays were performed by using single concentrations of other agents [0 mM Na^+, 1 mM phloretin (Pt), 100 mM L-fucose, 10 mM 2-deoxyglucose (2DG), 10 mM α-methyl-glucose (AMG)] and are presented in a bar graph. Data represent means ± SE of triplicates. *$P < 0.05$ with respect to MI uptake in the absence of competitor (Ctrl).

effectors (DCI, glucose, and Pz). Figure 4 presents a typical displacement curve of radiolabeled MI (0.36 nM) uptake by increasing concentrations of cold substrate (up to 2 mM). Data can be satisfactorily fitted to a single-site equation, as is shown by the linearity of an Eadie-Hofstee plot presented in the inset (K_m value of 0.12 ± 0.05 mM and V_{max} of 98 ± 36 pmol/mg protein × 15 s). Efforts to fit kinetic data to a two-site equation failed to identify a credible secondary system, consistent with the existence of a single transport system for MI in these vesicles. Kinetic analysis was performed for 7 independent experiments, generating similar MI K_m values spanning between 67 and 283 μM with an average of 150 ± 40 μM. Experiments similar to those shown in Fig. 3 were used to determine affinities for DCI, glucose, and Pz. As experiments were performed under the same conditions as those for MI, the kinetic constants determined for MI in each experiment (see Fig. 4) were used as constants here. As seen in Table 1 DCI exhibits a K_i value (146 ± 9 μM) similar to that of MI whereas the glucose K_m is sixfold higher (0.93 ± 0.35 mM). On the other hand, Pz is a potent inhibitor with a K_i of 15 ± 6 μM.

Characterization of Rat SMIT2 Expressed in Xenopus Oocytes

Rat SMIT2 was expressed in *Xenopus* oocytes to assess kinetic parameters for substrates (MI, DCI, and glucose) and an inhibitor (Pz) specifically for the rat SMIT2 protein, as determined in a heterologous system, and compare them to values obtained from rat intestinal BBMv. Figure 5*A* depicts current-voltage curves generated by plotting the oocyte current caused by the addition of MI (0–1 mM) at different membrane potentials. The currents elicited by MI at a given membrane potential were then plotted against the corresponding MI concentrations to determine the affinity for this substrate (Fig. 5*B*). The same approach was used to determine the affinities for the two other substrates: DCI (up to 1 mM) and glucose (up to 50 mM). Similarly, the K_i value for Pz was determined by fitting the currents induced by 0.1 mM MI in the presence of different Pz concentrations. For this purpose, the kinetic values (K_m and I_{max}) determined for MI (see Fig. 5*B*) were used as constants in

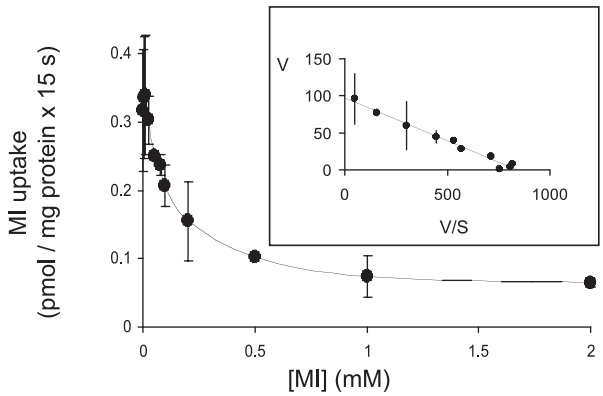

Fig. 4. Kinetic determination of MI transport into purified rat BBMv. Purified BBMv were incubated for 15 s with tracer MI (0.36 nM) in the presence of different concentrations of cold MI (up to 2 mM). Data were fitted according to Malo and Berteloot (28) using a tracer inhibition equation to obtain K_m and V_{max} values. The *inset* presents Eadie-Hofstee transformation of the data according to kinetic evaluation [nonspecific fraction of uptake (K_d) was removed] where V represents uptakes in pmol/mg protein × 15 s. Data are means ± SE of 4 determinations.

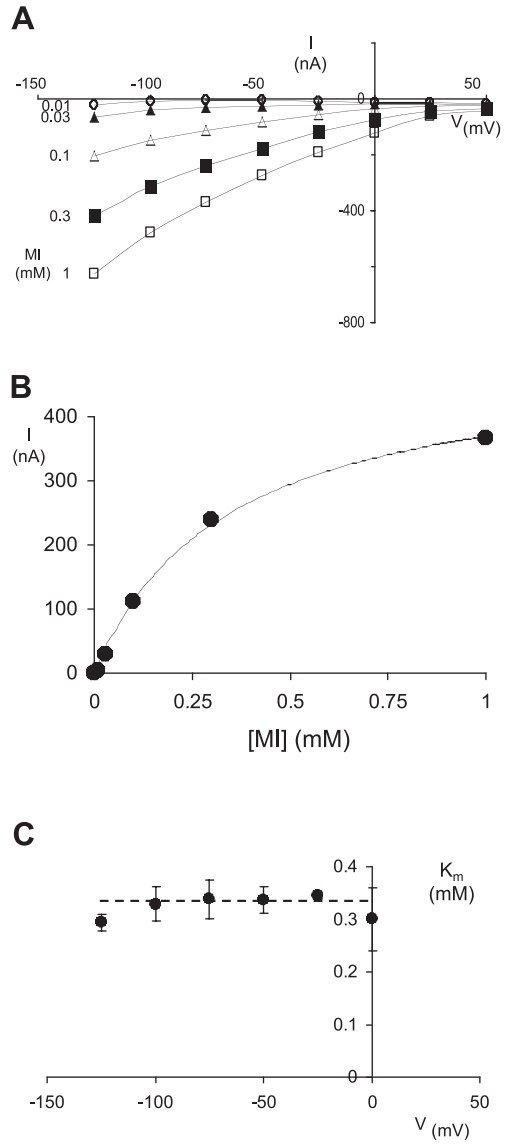

Fig. 5. Kinetic determination of MI transport into SMIT2-expressing oocytes. Oocytes were injected with 4.6 ng rat SMIT2 cRNA and tested for MI-specific currents after 5–7 days of incubation. *A*: *I*-V curves presenting currents (*I*) elicited by the addition of different concentrations of MI (0–1 mM) at membrane potentials spanning from +50 to −125 mV. Data presented are from a representative oocyte. *B*: current-vs.-MI concentration plot with values extracted from *A* at −50 mV. Data were used for the determination of kinetic parameters $K_m = 0.34 \pm 0.05$ mM, $I_{max} = 495 \pm 27$ nA. Data presented are from a unique oocyte. *C*: currents depicted in *A* were used to determine K_m values (as in *B*) at varying membrane potentials from −125 mV to 0 mV. The dashed line represents the mean of all K_m values for this oocyte.

a competitive inhibition equation to properly evaluate the K_i value of Pz. The K_m values remained fairly constant at different membrane potentials (see Fig. 5*C*). All kinetic parameters determined on oocytes are presented in Table 1 along with those already determined in BBMv. The kinetic parameters evaluated in oocytes showed similar affinities for MI (270 ± 19 μM), DCI (310 ± 56 μM) and Pz (16 ± 7 μM) to those measured in BBMv whereas the glucose affinity constant in oocytes is remarkably high (35.5 ± 7.3 mM), ~40 times higher than that seen with BBMv.

Table 1. *Kinetic parameters for MI uptake in rat BBMv and rat SMIT2-expressing oocytes*

	BBMv	Oocytes
MI	150±40 μM	270±19 μM
DCI	146±9 μM	310±56 μM
Glucose	930±350 μM	35,500±7,300 μM
Pz	15±6 μM	16±7 μM

Values are means ± SE. Kinetic parameters (K_m) were determined for various substrates [myo-inositol (MI), D-chiro-inositol (DCI), glucose] and an inhibitor [phlorizin (Pz)] using brush border membrane vesicles (BBMv) as well as *Xenopus laevis* oocytes. Evaluation of uptake into BBMv were performed as previously described (28) whereas oocytes currents were analyzed by classical equations (Michaelis-Menten and competitive inhibition).

Comparing Glucose and MI Transport in Purified Rat BBMv

To compare the activity levels of SMIT2 and SGLT1 in rat BBMv, tracer MI uptakes were compared with tracer glucose uptakes using the same vesicle preparations and the fast sampling rapid filtration apparatus. Figure 6 presents initial uptakes (up to 10 s) for both MI (●) and glucose (○) set at 0.4 nM along with linear regression analysis performed on the data to evaluate initial uptake capacities. As seen in this figure, tracer glucose uptake (0.0185 pmol/min) is sixfold higher than that found with MI (0.0033 pmol/min). Very similar ratios were found within all assays performed ($n = 5$). Given the low substrate concentrations used, the affinities of the two transporters for their substrates are unimportant and the data represent the true relative amounts of transport activity.

GLUT2 as a Basolateral Exit Pathway for MI

Because nutrients absorbed by enterocytes usually leave the cell through specific basolateral transport systems, we tested the possibility that GLUT2, the only basolateral pathway for glucose, could mediate the exit of MI. The human GLUT2 transporter was thus expressed in *X. laevis* oocytes and tested for the specific uptake of radiolabeled MI. As seen in Fig. 7, GLUT2 is unable to mediate MI transport, because barely any specific accumulation of MI is observed. On the other hand, 2DG, a specific substrate for GLUT2, was transported with great efficacy, as shown by the 67-fold increase in uptake of radiolabeled substrate in GLUT2-injected oocytes over that for control oocytes.

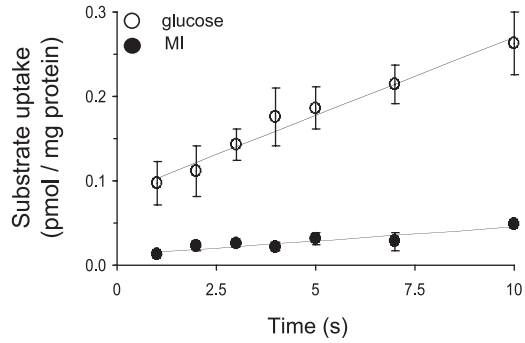

Fig. 6. Rapid MI uptake into purified BBMv. Purified rat BBMv were incubated for short time periods (up to 10 s) with tracer quantities of MI (●) or glucose (○). Initial uptake rates were determined from linear regression of the data for both MI (0.0033 pmol/min) and glucose (0.0185 pmol/min). Data represent means ± SE of triplicates.

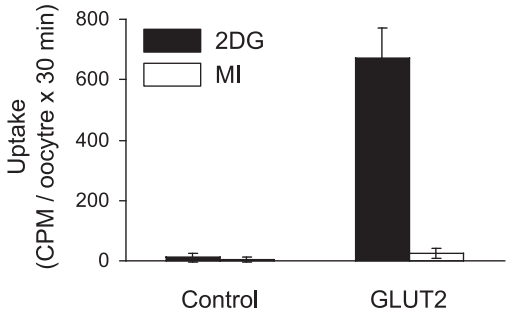

Fig. 7. MI and 2DG uptakes in GLUT2-expressing oocytes. Oocytes were injected with 46 ng of human GLUT2 cRNA and tested for both 2DG-specific (solid bars) and MI-specific (open bars) uptakes after 5–7 days of incubation. For both MI and 2DG, oocytes were incubated for 30 min in presence of either tracer alone or tracer with excess cold substrate (10 mM). The values represent the specific fraction of uptake as calculated by subtracting uptakes under saturating conditions to those determined with tracer alone. Data represent means ± SE of 6–10 oocytes per condition. Control oocytes were not injected.

DISCUSSION

In a previous report (24), we presented a complete characterization of MI transport in purified BBMv isolated from rabbit kidney in which we concluded that SMIT2 is responsible for the reuptake of MI from the kidney ultrafiltrate. Extending this study to intestinal tissue was a logical step because both tissues share obvious functional similarities. Initial studies performed on rabbit intestinal BBMv did not, however, show any evidence for the existence of a MI transport system, as shown in Fig. 1*A*. This difference between rabbit and rat can tentatively be explained by the fact that almost all of the rabbit dietary MI is found as phytate, a hexakisphosphate derivative of MI which essentially functions as a metal ligand in plants (17, 18). In contrast, free MI is by far the major form of inositol found in the rat diet (19). It was thus not surprising to find MI transport in intestinal BBMv isolated from rat, as seen in Fig. 1*B*, and no corresponding uptake in rabbit vesicles (Fig. 1*A*). However, a study showing the existence of a Na^+-dependent MI transport system in an herbivorous fish indicates that herbivores do not always lack Na^+/MI cotransport (35). Figure 1*B* demonstrates a classical overshoot of MI uptake that rapidly subsides within a few minutes, indicative of secondary active MI uptake. A similar assay performed in the presence of saturating MI (○) only showed equilibration of the substrate. This data is very similar to that already observed with BBMv purified from rabbit kidney (24). This species difference for SMIT2 expression in intestine is corroborated by qRT-PCR data (Fig. 2) indicating that SMIT2 transcripts are essentially absent from rabbit enterocytes and are not simply located in other cellular compartments (as is seen with GLUT4, which is located within intracellular stores when not needed) (31). In fact, the existence of a Na^+-dependent MI transport system in the rat intestine had already been demonstrated in purified BBMv (34), although without extensive characterization of the transport system(s) involved. We further pursued this investigation in rat BBMv to better characterize this activity in regards to its molecular identity and transport properties.

Characterization of MI transport performed through inhibition assays (Fig. 3) enabled us to identify the transport protein involved in this process. Using DCI and L-fucose as discriminating substrates for the two SMITs, we showed that only SMIT2 mediates MI transport in rat intestinal BBMv (Fig. 3), because DCI completely inhibited transport whereas 100 mM L-fucose failed to significantly alter MI uptake. Although complete inhibition of mediated MI transport by DCI is sufficient to identify SMIT2 as the unique transport system in this tissue, two other sugar transport systems that are present in the BBMv were also considered. First, the possible involvement of the fructose-specific transporter GLUT5 in MI transport was refuted since 2DG, a specific substrate for GLUTs including rat GLUT5 (32), did not alter the uptake of tracer MI even at 10 mM (Fig. 3, *bottom*). Also, because all MI transport was Na^+ dependent, as seen by the complete dissipation of mediated uptake when Na^+ is replaced by isosmolar K^+ (0 Na^+), any involvement of GLUT proteins or HMIT could be excluded since they all are Na^+ independent. The second system considered, the Na^+-glucose transporter SGLT1, was also ruled out since 10 mM AMG failed to significantly inhibit tracer MI uptake. The use of 10 mM AMG as a specific condition for evaluating the possible contribution of SGLT1 to MI uptake was justified by the fact that this concentration is much higher than the K_m of this specific substrate for SGLT1 (0.4 mM; Ref. 25) yet it does not appear to affect cloned rabbit SMIT2 (10). In addition, rat SMIT2 has even less affinity for AMG than does the rabbit protein since AMG superfusion could not elicit any current in oocytes expressing rat SMIT2, even at 50 mM (R. Aouameur, unpublished observation). Finally, as expected for a Na^+-dependent sugar transport system, SMIT2 shows great affinity toward Pz (15 ± 6 μM). The K_m value found for MI with rat BBMv (150 ± 40 μM) is comparable to that found by Scalera et al. on a similar preparation (34) or to that found using rabbit kidney BBMv (15, 24).

When comparing the various kinetic parameters described for SMIT2 between the oocyte expression system and BBMv, the single noteworthy difference concerns the affinity for glucose. Although the glucose affinity found for rat SMIT2 expressed in oocytes (mean K_m value of 4 assays = 35.5 ± 7.3 mM) is compatible with the affinities previously reported for rabbit SMIT2 (10), the K_i values found in BBMv assays are remarkably lower (mean value of 4 assays = 0.93 ± 0.35 mM). A possible role for SGLT1 activity in affecting measurements of glucose inhibition of SMIT2, such as rapid dissipation of sodium gradient or reduced membrane potential, is unlikely since a high concentration of AMG (10 mM) did not significantly alter tracer uptake of MI. Also, as seen in Fig. 5*C*, the K_m for SMIT2 is not influenced by more positive membrane potentials, indicating that a change in membrane potential should not reduce MI uptake. We cannot rule out the possibility that SGLT1 is involved in the unusually low K_i value for glucose inhibition of SMIT2, but any actual mechanism must be more complex than simple competitive inhibition. To sum up the comparisons, although MI and DCI compete the transport of radiolabeled MI with K_i values that are consistent with their measured K_m in oocytes and Pz inhibits radiolabeled MI uptake in BBMv with a K_i value that is also observed in electrophysiological experiments, the observed K_m value for D-glucose-induced current is 40 times larger than the K_i observed in BBMvs. This indicates that the mechanism used for inhibition is different from the mechanism used for transport. The difference maybe that in oocyte SMIT2 is alone but in BBMv, the activity of SMIT2 is measured in the presence of an intense transport activity mediated by SGLT1. Inhibition of SMIT2 must involve a site separate from that required for

cotransport, which may be inside or outside the membrane, and will require future study. Our data appear to be in agreement with the study from Scalera et al. (34) evaluating MI uptake in rat BBMv, where glucose was shown to be an inhibitor with mixed-type mechanism and with very weak transport efficiency.

Many reports have stressed the dietary need for MI. Studies in gerbils have linked intestinal MI uptake to lipid metabolism and chylomicron synthesis because its removal from the diet was shown to generate pathological conditions such as intestinal lipodystrophy and liver dysfunction of lipid metabolism (5–8, 18, 19). Because MI metabolism seems to occur within enterocytes (19), the existence of a basolateral pathway for its exit may not be required as it is for other absorbed nutrients such as glucose although there is evidence of ingested MI appearing in both mouse and human plasma (3, 14). In fish, however, there is a single report presenting data for a basolateral pathway for MI (33) and, as expected, this transport is diffusive (Na^+ independent). In mammals, on the other hand, GLUT2 is the basolateral pathway responsible for the exit of glucose from enterocytes and proximal convoluted tubule (kidney) cells. Consequently, we examined the possibility that this sugar transporter could mediate MI transport but no specific uptake was observed when this transporter was expressed in oocytes (Fig. 7). Assays using purified basolateral membranes to identify a specific pathway for MI exit are presently underway in our laboratory.

Comparing the uptake of glucose and MI into BBMv shows that SGLT1 activity is about six times stronger than SMIT2 activity (Fig. 6). When considering that the K_m value for intestinal glucose transport on SGLT1 (140 μM; Ref. 29) is very similar to that for MI determined on SMIT2 (150 μM, herein), it can be concluded that SGLT1 glucose transport activity should be six times larger that of SMIT2 in the rat intestine for equimolar concentrations of glucose and MI. With its very weak affinity for glucose, a significant participation of SMIT2 in intestinal glucose uptake seems unlikely. This is corroborated by the glucose-galactose malabsorption syndrome in humans, characterized by a deficit in SGLT1 function, which is not obviously compensated for by the presence of SMIT2. Evaluation of competition between the two substrates for SMIT2 transport is largely meaningless in the absence of fixed luminal glucose and MI concentrations. In kidney, where both transporters are also found and glucose and MI concentrations are stable, such consideration becomes relevant but will depend on the specific intranephronic location of MI and glucose cotransporters (24).

In conclusion, we have presented evidence for SMIT2-dependent uptake of MI in the apical domain of rat enterocytes similar to those already determined in rabbit kidney (24).

GRANTS

This work was supported by the Canadian Institutes of Health Research (CIHR), grant no. MOP-67038.

REFERENCES

1. **Berteloot A, Malo C, Breton S, Brunette M.** Fast sampling, rapid filtration apparatus: principal characteristics and validation from studies of D-glucose transport in human jejunal brush-border membrane vesicles. *J Membr Biol* 122: 111–125, 1991.
2. **Bissonnette P, Coady MJ, Lapointe JY.** Expression of the sodium-myo-inositol cotransporter SMIT2 at the apical membrane of Madin-Darby canine kidney cells. *J Physiol* 558: 759–768, 2004.
3. **Chau JF, Lee MK, Law JW, Chung SK, Chung SS.** Sodium/myo-inositol cotransporter-1 is essential for the development and function of the peripheral nerves. *FASEB J* 19: 1887–1889, 2005.
4. **Chen XZ, Coady MJ, Jalal F, Wallendorff B, Lapointe JY.** Sodium leak pathway and substrate binding order in the Na^+-glucose cotransporter. *Biophys J* 73: 2503–2510, 1997.
5. **Chu SH, Geyer RP.** Myo-inositol action on gerbil intestine: reversal of a diet-induced lipodystrophy and change in microsomal lipase activity. *Biochim Biophys Acta* 664: 89–97, 1981.
6. **Chu SH, Geyer RP.** Tissue content and metabolism of myo-inositol in normal and lipodystrophic gerbils. *J Nutr* 113: 293–303, 1983.
7. **Chu SH, Hegsted DM.** Myo-inositol deficiency in gerbils: comparative study of the intestinal lipodystrophy in *Meriones unguiculatus* and *Meriones libycus*. *J Nutr* 110: 1209–1216, 1980.
8. **Chu SW, Geyer RP.** myo-Inositol action on gerbil intestine. Association of phosphatidylinositol metabolism with lipid clearance. *Biochim Biophys Acta* 710: 63–70, 1982.
9. **Clements RS Jr, Diethelm AG.** The metabolism of myo-inositol by the human kidney. *J Lab Clin Med* 93: 210–219, 1979.
10. **Coady MJ, Wallendorff B, Gagnon DG, Lapointe JY.** Identification of a novel Na^+/myo-inositol cotransporter. *J Biol Chem* 277: 35219–35224, 2002.
11. **Dawson RM, Freinkel N.** The distribution of free mesoinositol in mammalian tissues, including some observations on the lactating rat. *Biochem J* 78: 606–610, 1961.

11a. **Dmitrieva NI, Burg MB.** Osmotic stress and DNA damage. *Methods Enzymol* 428: 241–252, 2007.

12. **Dolhofer R, Wieland OH.** Enzymatic assay of myo-inositol in serum. *J Clin Chem Clin Biochem* 25: 733–736, 1987.
13. **Gagnon MP, Bissonnette P, Deslandes LM, Wallendorff B, Lapointe JY.** Glucose accumulation can account for the initial water flux triggered by Na^+/glucose cotransport. *Biophys J* 86: 125–133, 2004.
14. **Groenen PM, Merkus HM, Sweep FC, Wevers RA, Janssen FS, Steegers-Theunissen RP.** Kinetics of myo-inositol loading in women of reproductive age. *Ann Clin Biochem* 40: 79–85, 2003.
15. **Hammerman MR, Sacktor B, Daughaday WH.** myo-Inositol transport in renal brush border vesicles and it inhibition by D-glucose. *Am J Physiol Renal Fluid Electrolyte Physiol* 239: F113–F120, 1980.
16. **Handler JS, Kwon HM.** Regulation of renal cell organic osmolyte transport by tonicity. *Am J Physiol Cell Physiol* 265: C1449–C1455, 1993.
17. **Haydon MJ, Cobbett CS.** Transporters of ligands for essential metal ions in plants. *New Phytol* 174: 499–506, 2007.
18. **Holub BJ.** Metabolism and function of myo-inositol and inositol phospholipids. *Annu Rev Nutr* 6: 563–597, 1986.
19. **Holub BJ.** The nutritional significance, metabolism, and function of myo-inositol and phosphatidylinositol in health and disease. *Adv Nutr Res* 4: 107–141, 1982.
20. **Ibsen L, Strange K.** In situ localization and osmotic regulation of the Na^+-myo-inositol cotransporter in rat brain. *Am J Physiol Renal Fluid Electrolyte Physiol* 271: F877–F885, 1996.
21. **Kaluz S, Kolble K, Reid KB.** Directional cloning of PCR products using exonuclease III. *Nucleic Acids Res* 20: 4369–4370, 1992.
22. **Kwon HM, Yamauchi A, Uchida S, Preston AS, Garcia-Perez A, Burg MB, Handler JS.** Cloning of the cDNa for a Na^+/myo-inositol cotransporter, a hypertonicity stress protein. *J Biol Chem* 267: 6297–6301, 1992.
23. **Lahjouji K, Aouameur R, Bissonnette P, Coady MJ, Bichet DG, Lapointe JY.** Expression and functionality of the Na^+/myo-inositol cotransporter SMIT2 in rabbit kidney. *Biochim Biophys Acta* 1768: 1154–1159, 2007.
24. **Lahjouji K, Aouameur R, Bissonnette P, Coady MJ, Bichet DG, Lapointe JY.** Expression and functionality of the Na^+/myo-inositol cotransporter SMIT2 in rabbit kidney. *Biochim Biophys Acta* 1768: 1154–1159, 2007.
25. **Lee WS, Kanai Y, Wells RG, Hediger MA.** The high affinity Na^+/glucose cotransporter. Re-evaluation of function and distribution of expression. *J Biol Chem* 269: 12032–12039, 1994.
26. **Lien YH, Shapiro JI, Chan L.** Effects of hypernatremia on organic brain osmoles. *J Clin Invest* 85: 1427–1435, 1990.
27. **Lien YH, Shapiro JI, Chan L.** Study of brain electrolytes and organic osmolytes during correction of chronic hyponatremia. Implications for the pathogenesis of central pontine myelinolysis. *J Clin Invest* 88: 303–309, 1991.
28. **Malo C, Berteloot A.** Analysis of kinetic data in transport studies: new insights from kinetic studies of Na^+-D-glucose cotransport in human intestinal brush-border membrane vesicles using a fast sampling, rapid filtration apparatus. *J Membr Biol* 122: 127–141, 1991.

29. **Mate A, Barfull A, Hermosa AM, Gomez-Amores L, Vazquez CM, Planas JM.** Regulation of sodium-glucose cotransporter SGLT1 in the intestine of hypertensive rats. *Am J Physiol Regul Integr Comp Physiol* 291: R760–R767, 2006.
30. **Pascual JM, Solivera J, Prieto R, Barrios L, Lopez-Larrubia P, Cerdan S, Roda JM.** Time course of early metabolic changes following diffuse traumatic brain injury in rats as detected by (1)H NMR spectroscopy. *J Neurotrauma* 24: 944–959, 2007.
31. **Pessin JE, Bell GI.** Mammalian facilitative glucose transporter family: structure and molecular regulation. *Annu Rev Physiol* 54: 911–930, 1992.
32. **Rand EB, Depaoli AM, Davidson NO, Bell GI, Burant CF.** Sequence, tissue distribution, and functional characterization of the rat fructose transporter GLUT5. *Am J Physiol Gastrointest Liver Physiol* 264: G1169–G1176, 1993.
33. **Reshkin SJ, Vilella S, Ahearn GA, Storelli C.** Basolateral inositol transport by intestines of carnivorous and herbivorous teleosts. *Am J Physiol Gastrointest Liver Physiol* 256: G509–G516, 1989.
34. **Scalera V, Natuzzi D, Prezioso G.** myo-inositol transport in rat intestinal brush border membrane vesicles, and its inhibition by D-glucose. *Biochim Biophys Acta* 1062: 187–192, 1991.
35. **Vilella S, Reshkin SJ, Storelli C, Ahearn GA.** Brush-border inositol transport by intestines of carnivorous and herbivorous teleosts. *Am J Physiol Gastrointest Liver Physiol* 256: G501–G508, 1989.
36. **Wood IS, Trayhurn P.** Glucose transporters (GLUT and SGLT): expanded families of sugar transport proteins. *Br J Nutr* 89: 3–9, 2003.
37. **Wright EM, Hirayama BA, Loo DF.** Active sugar transport in health and disease. *J Intern Med* 261: 32–43, 2007.
38. **Yamashita T, Shimada S, Yamauchi A, Guo W, Kohmura E, Hayakawa T, Tohyama M.** Induction of Na^+/myo-inositol co-transporter mRNA after rat cryogenic injury. *Brain Res Mol Brain Res* 46: 236–242, 1997.
39. **Yamauchi A, Kwon HM, Uchida S, Preston AS, Handler JS.** Myo-inositol and betaine transporters regulated by tonicity are basolateral in MDCK cells. *Am J Physiol Renal Fluid Electrolyte Physiol* 261: F197–F202, 1991.